A study on mechanism of flame acceleration of H_2/C_3H_8-Air mixtures in an obstructed square channel

Guanbing CHENG[1,2], Ratiba ZITOUN[2], Yves SARRAZIN[2], Pascal BAUER[2], Pièrre VIDAL[2]

[1]Aeronautical Engineering College, Civil Aviation University of China, No.2898, Jinbei Road, Dongli District, 300300 Tianjin, P R China

[2]Institut P' UPR 3346, Département Fluides, Thermique, Combustion, CNRS
1 Av. Clément Ader, BP 40109, 86961 FUTUROSCOPE CEDEX, FRANCE

1 Introduction

Because of the increasing consumption of fossil fuels and associated environmental concerns, more attention is being paid on hydrogen industry. Since its combustion products do not contain hydrocarbons (HC) and carbon dioxide (CO_2), hydrogen is regarded as an alternative energy carrier. However, its lower ignition energy, wider flamability concentration limits and higher ability for leakage make the potential explosion hazards possible in terms of the industrial stockage, transportation and distribution [1]. Cheng et al.[2-3] found that the addition of a small amount of propane to the H_2/Air mixtures provided an increase of the detonation cell size, i.e. from 10 mm to 50 mm in the stoichmetric conditions, when the molar fraction of propane in the binary fuels H_2/C_3H_8 varied from 0 to 0.7. The hydrogen industrial hazardous scenario are generally related to the onset of detonation or **deflagration-to-detonation transition** (**DDT**) following the flame acceleration in certain extreme cases[3-5]. Hence, it is of particular importance to examine the mechanism of flame acceleration in such binary fuels H_2/C_3H_8-Air mixtures.

An attempt is made in the paper to identify the physical mechanisms of flame propagation of H_2/C_3H_8-Air mixtures in a square channel equipped with different obstacles. All the experiments are carried out at normal pressure and temperature conditions in the channel filled with mixtures at equivalence ratio Φ=1.1 and molar fraction of hydrogen x=0.9. The mixture compositions are given by: Φ [x H_2+ (1-x) C_3H_8] + (5–4.5x) (O_2 + 3.76 N_2); $x = H_2/(H_2 + C_3H_8)$.

2 Experimental facilities

A sketch of the experimental setups is presented in Fig.1. All the experiments are performed in a stainless-steel square channel with 40-mm×40-mm square cross-section and 4-m length. The channel consists of 8 50-cm length sections. Two optical sections located at the beginning of the tube are equipped with glass windows on both sides in order to visualize the flame propagation. Each section has two instrumentation ports to equipped with pressure transducers. Nine piezoelectric pressure transducers (KISTLER 603B, 1 μs rise time) are distributed along the channel to obtain the pressure-time records. The first transducer is placed at 37.5 cm from the spark plug on the first optical section, whereas another port is used to evacuate/fill the mixtures in the channel. The studied mixtures (Φ=1.1, x=0.9) are ignited by an automotive spark plug with about 15-mJ energy discharge. An array of periodical obstacles located along the first half of the total channel is used to accelerate the flame. Three different obstacles, namely perforated orifice plates (Obstacle 1), plane plates (Obstacle 2) and Schelkin spiral (Obstacle 3), with a pitch equal to the channel height and a blockage ratio BR=0.5 are utilized in the experiments. The obstacle geometrical characteristics are presented in detail in Tab. 1. In addition, a typical Z-shadow system is shown in Fig.2 to visualize the flame propagation or the DDT phenomenon. The optical setup is made of a 500-Watt mercury vapor arc lamp (HC500W2O), two 45-cm diameter, 4-m focal length parabolic mirrors, and two ultra speed digital cameras. The camera shutter time varies from 1µs to 250 ns, over a frequency ranging from 32000 to1000000, respectively.

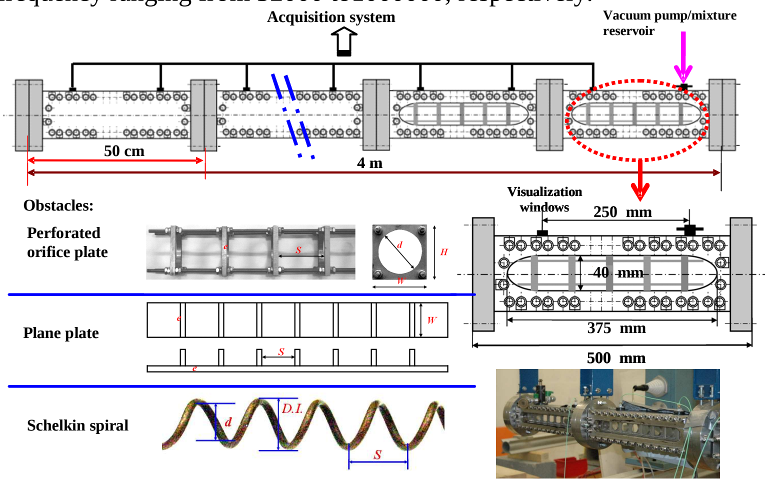

Figure 1. Schema of experimental facilities

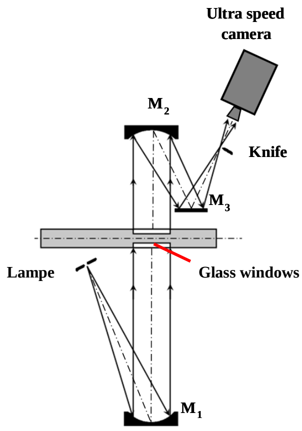

Figure 2. A typical Z-shadow system

Table 1. Geometrical characteristics of different obstacles in the channel

Obstacle type	*W=H* mm	*d* mm	*D.I mm*	*S* mm	*L* m	*e* mm
Perforated orifice plate	40	31	/	40	1.7	4
Flat plate	40	/	/	40	1.4	6
Schelkin Spiral	/	24	40	40	2.0	8

3 Results and discussion

3.1 Obstacle 1: Perforated orifice plates

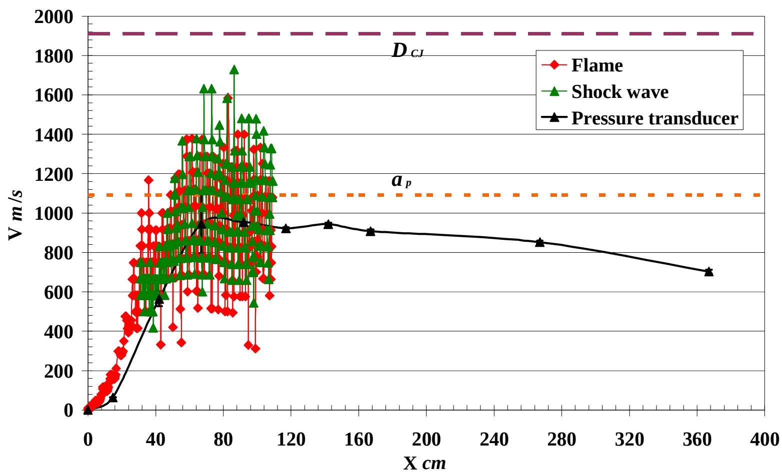

Figure 3. Evolution of the flame, shock precursor velocities measured by the pressure transducer and the shadow method with the distance along the tube for the studied mixtures (Φ=1.1, x=0.9)-Obstacle 1: S=40 mm, e=4 mm, L=1.7 m

The evolution of the flame, shock precursor velocities is shown in Fig.3 as a function of distance X from the ignition point for the mixtures in the channel equipped with perforated orifice plates (obstacle 1). The black dots represent the average velocities of the front derived from pressure transducers, whereas the red or green points correspond the flame or shock precursor average velocities measured by the shadow method. From Fig.3, two stage of flame acceleration, namely the front velocity lower or higher than the unreactant sound speed defined in [6], are observed. One can observe that the flame velocities measured by the photographic method are slightly higher than that those derived from pressure transducers measurements. This can be explained by the distance between the first transducer and the spark plug which is on the order of 37 cm. A shock wave can be observed at the end of the 1st section. The choking flame can be nearly reached at the second pressure transducer. DDT has not been observed for the studied mixtures. At the first stage of flame propagation, the compressibility effects play a minor role. The evolution of the flame front surface, the expansion of the combustion product and the delayed combustion between the two adjacent plates play a major role in the flame acceleration. An example of the flame-shock fronts crossing the 8th obstacle is exhibited in Fig. 4. On the basis of our experimental results, the interactions between the flame front and the shock reflection on the surface of either the channel or the plates are the primary mechanisms for the second stage of flame acceleration.

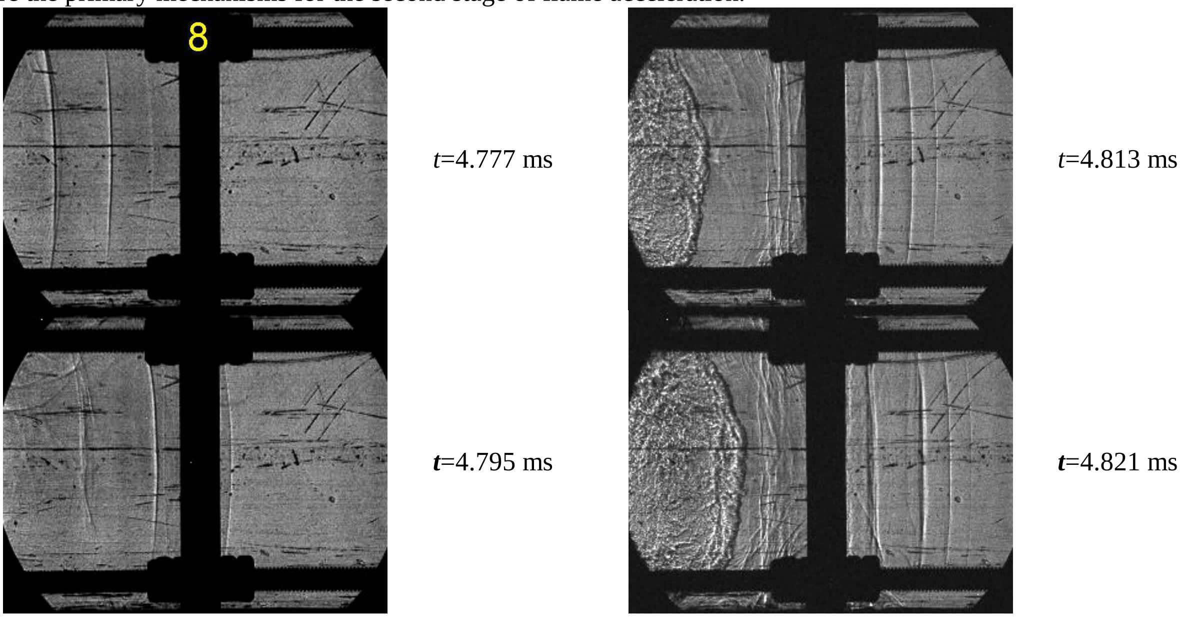

Figure 4. Example of flame-shock propagation in the 8th obstacle (mixtures at Φ=1.1, x=0.9) Obstacle 1-S=40 mm, e=4 mm, L=1.7 m

3.2 Obstacle 2: Plane plates

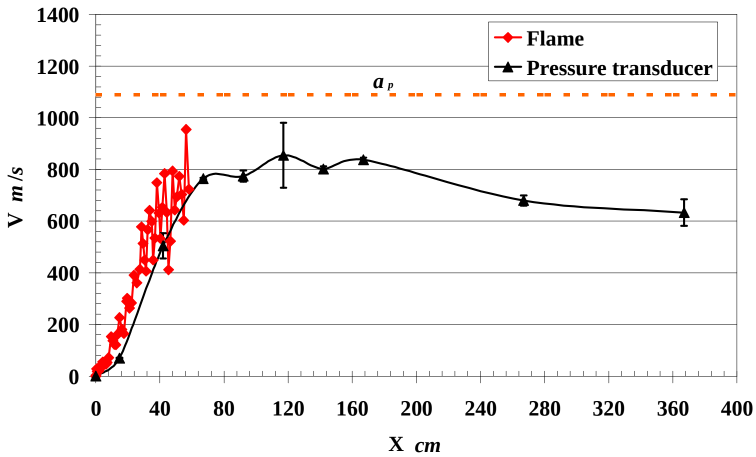

Figure 5. Evolution of the front average velocities measured by the pressure transducer and the shadow method *vs*. the distance along the tube (mixtures Φ=1.1, x=0.9)-Obstacle 2:S=40 mm, e=6 mm, L=1.4 m

The evolution of the flame, shock average velocities derived from pressure transducers and the photographic method along the distance X from the spark plug is shown in Fig.5. The flame velocities in red points are measured by the shadow method in the central axial direction of the opening of the channel. It has been observed that the flame velocities obtained by the Schlieren method are higher that those derived from the pressure transducers. The flame does not reach the choking regime. The mechanisms for the two stages of flame propagation in the channel with obstacle 2 are similar to those observed with the perforated orifice plates.

An example of flame, precursor shock diffraction around the obstacle at a distance of 1.2 m from the ignition point is shown in Fig.6. From Fig.6, one can observe that there is a complex shock system when the precursor shock diffracts around the obstacle. The reflected shocks from the inner surfaces of the channel interact with those reflected from the upstream surface of the obstacle and the flame front. At *t*=5.212 ms, a hot spot is seen at the corner, but the onset of detonation can not be successfully observed.

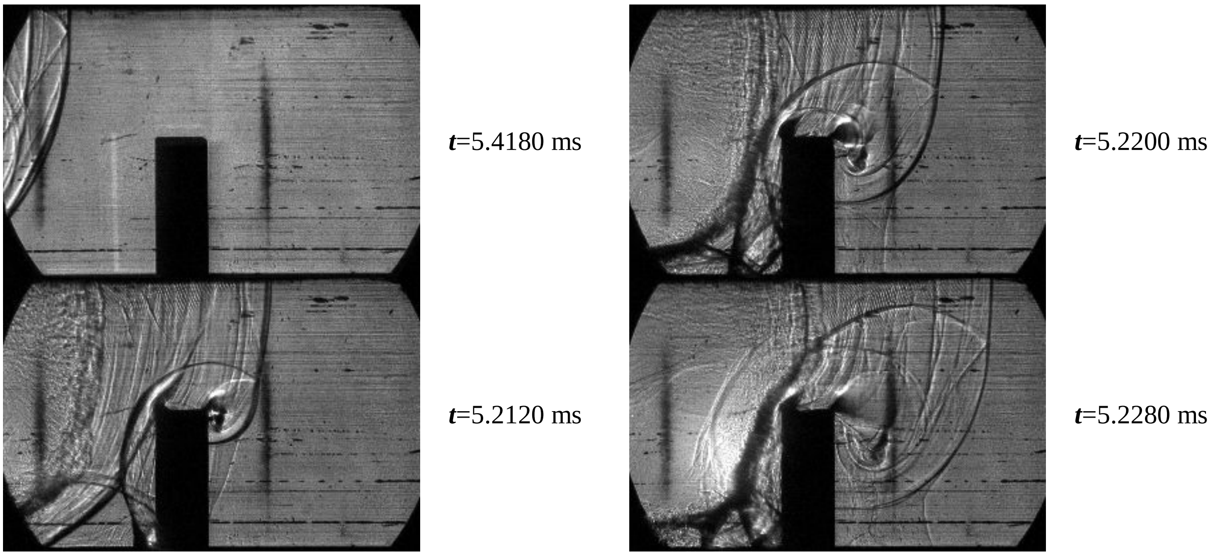

Figure 6. Example of flame-shock diffraction around an obstacle of the studied mixtures (Φ=1.1, *x*=0.9) at the distance of the order of 1.2 m from the ignition point-Obstacle 2-*S*=40 mm, *e*=6 mm, *L*=1.4 m

3.3 Obstacle 3: Schelkin spiral

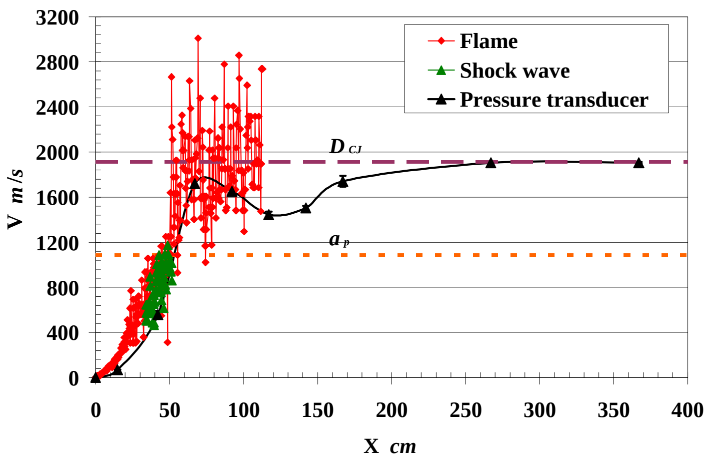

Figure 7. Variations of the flame, shock, detonation average velocities measured by the pressure transducer and the shadow method along the distance X along the tube (mixtures Φ=1.1, *x*=0.9)-Obstacle 3:*S*=40 mm, *e*=8 mm, *L*=2.0 m

With the help of the pressure transducers (black points) and the ultra-speed camera (red and green points corresponding the flame and shock precursor velocity, respectively), the variations of the measured central flame, shock wave, and detonation wave average velocities are shown in Fig. 7. The variations of flame-shock propagation along the Schelkin spiral are exhibited in Fig.8. One can observe in Figs.7 and 8 that the front average velocities measured by the shadow method are higher than those derived from the pressure transducers. Likewise it was observed in obstacle 1, the shock wave has been recorded at the end of the channel (as it shows in second image of Fig.8). The increases of flame surface as well as the combustion product expansion are gouverning the first stage of flame propagation. The shock reflected from the surface of spiral is the main factor for the second stage of flame acceleration. Experimental results involving the obstacle 3 show that the run-up distance to DDT observed at the end of the 13th chamber is on the order of the 54 cm. This is based on the method of photographic, which is similar to 60 cm measured by the pressure transducers.

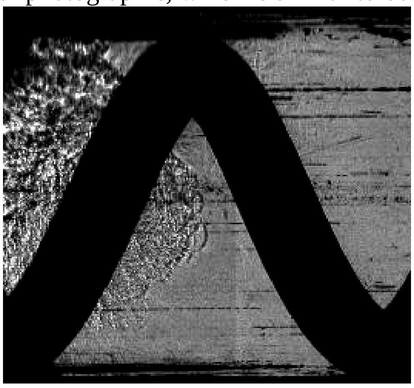

t=4.512 ms in the 8th chamber

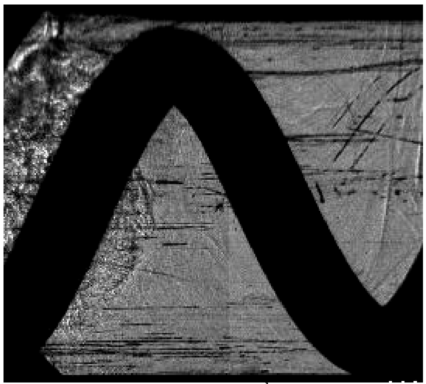

t=4.556 ms in the 9th chamber

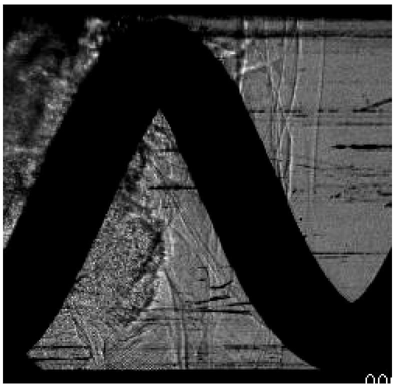

t=4.598 ms in the 10th chamber

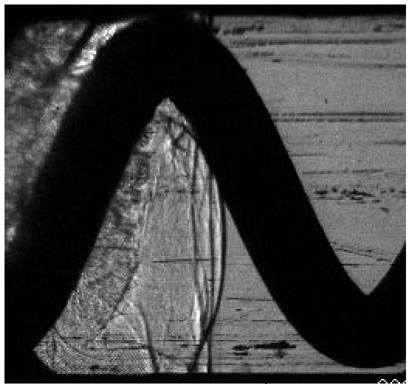

t=4.626 ms in the 11th chamber

Figure 8. Example of flame-shock propagation along the tube equipped with the Schelkin spiral for the studied mixtures (Φ=1.1, x=0.9) in the 8th -11th chambers from the ignition point-Obstacle 3-S=40 mm, e=8 mm, L=2.0 m (the length of each chamber equals to the spiral pitch, S=$D.I$)

4 Conclusions

An experimental study of the physical mechanisms of the flame acceleration in binary fuels hydrogen (H_2)/propane (C_3H_8)-Air mixtures (Φ=1.1, x=0.9) is carried out. All the experiments are performed in a stainless steel square channel tube of 40-mm×40-mm square cross-section and 4-m length. Three different obstacles (perforated orifice plate, plane plate and Schelkin spiral) are used to promote the flame acceleration or even the onset of detonation. The physical mechanisms of flame acceleration are discussed on the basis of data derived from pressure transducers and ultra-speed camera records. The evolution of the flame front surface, the combustion product expansion and the delayed combustion between the two adjacent plates are the main factors for the first stage of flame propagation phenomenon. During its second stage, the interactions between the flame front and the shock reflection on the channel inner surface, or on the plate upstream surface, or the spiral surface, are the major mechanisms. When using the Schelkin spiral, the oscillations of the measured front velocities are less evident than those obtained in obstacles 2 and 3 in the first stage. The DDT phenomenon is observed at the end of the 13th chamber. The 54-cm run-up distance to DDT measured by ultra-speed camera is similar to that (60cm) obtained by means of the pressure transducers.

References

[1] D. Desbordes. (1986). Etude de la TDD. Report of LCD 1-86.

[2] G. Cheng, R. Zitoun, P. Bauer. (2011). Detonation characteristics in tube filled with the binary fuels H_2/C_3H_8-Air mixtures. Proc. 23rd ICDERS, Paper 129.

[3] G. Cheng, R. Zitoun, Y. Sarrazin, P. Bauer. (2011).Deflagration-detonation transition in tube filled with the binary fuels H_2/C_3H_8-Air mixtures. Proc. European Combustion Meeting, Cardiff.

[4] G. Cheng, R. Zitoun, Y. Sarrazin, P. Bauer. (2013).Enhancement of DDT in binary fuels H_2/C_3H_8-Air mixtures Application to Propulsion, Aerotecnica, in press.

[5] G.Cheng, R. Zitoun, Y. Sarrazin, P. Bauer, P. Vidal. (2013).A study on mechanism of the initial stage of flame propagation in the obstructed channel filled with H_2/C_3H_8-Air mixtures, Proc. 9th Aian-Pacific Conference on Combustion, Gyeongju, Korea.

[6] G. Ciccarelli, C.T. Johansen, M. Parravani. (2010), The role of shock-flame interactions on flame acceleration in an obstacle laden channel, Comb and Flame 157(2010) pp: 2125-2136